Check for updates

Received: 16 August 2022 | Revised: 1 November 2022 | Accepted: 23 November 2022

DOI: 10.1111/jace.18951

Journal of the American Ceramic Society

RESEARCH ARTICLE

Ink development for the additive manufacturing of strong green parts by layerwise slurry deposition (LSD-print)

Sarah Diener[1,3] | **Hendrik Schubert**[2] | **Jens Günster**[2,3] | **Andrea Zocca**[2]

[1]Kyocera Fineceramics Precision GmbH, Selb, Germany

[2]BAM, Bundesanstalt für Materialforschung und -prüfung, Division Advanced Multi-materials Processing, Berlin, Germany

[3]Institute of Non-Metallic Materials, Clausthal University of Technology, Clausthal-Zellerfeld, Germany

Correspondence
Sarah Diener, Kyocera Fineceramics Precision GmbH,
Lorenz-Hutschenreuther-Str. 81, 95100 Selb, Germany.
Email:
sarah.diener@kyocera-precision.com

Funding information
AMITIE (Additive Manufacturing for Transnational Innovation in Europe); H2020-MSCA-RISE-2016 EU Research & Innovation Programe, Grant/Award Number: 734342; German Federal Ministry for Education and Research (BMBF), Grant/Award Number: 03XP0193

Abstract

Obtaining dense fine ceramics by the binder jetting additive manufacturing process is challenging. A slurry-based binder jetting process, such as the layerwise slurry deposition (LSD-print) process, can enable the printing of dense ceramic parts. This work describes a procedure to develop and qualify a suitable ink to manufacture silicon carbide green parts by LSD-print. Not only the printability but also the compatibility of the ink with the powder bed and the effect of the binding agent on the properties of the green parts are considered. Both aspects are important to obtain high green strength, which is necessary for printing large or thin-walled parts. Characterization methods, such as rheological and surface tension measurements, are applied to optimize three selected inks. The interplay between ink and powder bed is tested by contact angle measurements and by comparing the biaxial strength of cast and additively manufactured specimens. Out of the three binding agents tested, a polyethyleneimine and a phenolic resin have a high potential for their use in the LSD-print of silicon carbide green bodies, whereas a polyacrylate binding agent did not show the required properties.

KEYWORDS
binders/binding, inkjet, printing, silicon carbide

1 | INTRODUCTION

Binder jetting is an additive manufacturing method offering high productivity and scalability to very large build volumes. Parts are made by depositing a layer of powder followed by printing an ink to inscribe the cross section of the objects in every layer. Layer deposition and ink application are repeated until the desired parts are finished.[1] In this work, the term "ink" refers to the liquid that is printed into the powder bed through a printhead. The ink comprises a liquid vehicle, a binding agent, and often other additives. A curing step is often required to evaporate the liquid vehicle and harden the binding agent to provide sufficient green strength before the parts can be removed from the surrounding powder bed.[2] This de-powdering step is performed by compressed air and brushes to sweep away the loose powder. Due to the comparably low density of the powder bed, this can be done relatively easily. A challenge of powder-based binder jetting for fine ceramics is, however, the low packing density of the powder bed, which results in a low green density.[3] For this reason, modifications of the binder jetting process in which a

This is an open access article under the terms of the Creative Commons Attribution-NonCommercial-NoDerivs License, which permits use and distribution in any medium, provided the original work is properly cited, the use is non-commercial and no modifications or adaptations are made.
© 2023 The Authors. *Journal of the American Ceramic Society* published by Wiley Periodicals LLC on behalf of American Ceramic Society.

15512916, 0, Downloaded from https://ceramics.onlinelibrary.wiley.com/doi/10.1111/jace.18951 by Fak - Bam Berlin, Wiley Online Library on [04/01/2023]. See the Terms and Conditions (https://onlinelibrary.wiley.com/terms-and-conditions) on Wiley Online Library for rules of use; OA articles are governed by the applicable Creative Commons License

slurry is used instead of a powder have been proposed to increase the green density of the printed ceramic parts.[4] A variation of slurry-based binder jetting is the layerwise slurry deposition (LSD-print), in which a thin layer of slurry is spread utilizing a doctor blade and dried before the ink is applied.[5,6] This technology has been applied to different ceramic materials, such as alumina,[7] silicon infiltrated silicon carbide SiSiC,[8] and porcelain.[9]

The use of a slurry leads to a densely packed powder bed. The mechanism underlying particle packing has been modeled similarly to a slip-casting process in which the particles are drawn to the previous layers by capillary forces and can rearrange in the liquid medium during deposition.[9] Moreover, fine particle sizes can be used in the slurry, as opposed to powder bed processes in which usually coarser powders are needed to fulfill certain criteria regarding powder flowability. These advantages, however, come with the disadvantages of needing an extra drying step and of a more complex de-powdering.[10] Indeed, powder beds produced by LSD are so densely packed that the powder surrounding the printed parts has to be re-dispersed in water. This consideration implies that certain requirements of the ink and the powder bed are substantially different between powder-based binder jetting and LSD-print. Specifically, the parts printed in the LSD-print process must be water-insoluble to withstand the washing process, whereas the surrounding powder bed is re-dispersed in water. For the handling of large green parts, a high green strength is necessary to survive this washing step. On the other hand, the dense and rigid powder bed provides strong support to the printed parts, increasing the freedom in design without the necessity to consider the addition of support structures.

The interaction between ink and powder bed is a key factor that impacts the green strength of printed parts.[11] Both the compositions of the ink and the slurry need to be optimized to ensure a stable process, from droplet ejection, to contact and spreading in the powder bed, to the final adhesion properties. Ink selection procedures for the binder jetting process are well known in the literature.[12–14] However, ink printability and optimization of the printed parts are usually treated separately, thus missing an integral view of the whole process. In the LSD-print process, the interactions of ink and slurry are unique and even more complex than in powder-based binder jetting; thus, ink and ceramic slurry cannot be evaluated independently. In a previous work, we have shown how the slurry composition influences the powder-ink interaction.[11]

In this work, we consider the same issue from the perspective of the ink selection, keeping the slurry composition constant. Furthermore, as some requirements are unique to the LSD-print process, we present a dedicated ink selection procedure specific to this technology. Three inks are proposed and compared for the printing of silicon carbide green bodies. We have shown in a previous article that such green bodies manufactured by LSD-print can be infiltrated with liquid silicon to produce a high-quality silicon infiltrated silicon carbide material with a low amount of residual metallic silicon.[8]

2 | DESCRIPTION OF THE DEVELOPED INK SELECTION PROCEDURE

Figure 1 shows the flow diagram of the proposed procedure to optimize an ink for binder jetting. The peculiarities of the ink selection specifically for the LSD-print process, compared to powder-based binder jetting, are highlighted in red. The aim is to develop an ink that enables the printing of green parts with high green strength and resolution. Further processing steps, including debinding and silicon infiltration or sintering, are out of the scope of this work.

The ink typically comprises a liquid vehicle, a binding agent, and additives. Components, such as cosolvents, humectants, or surfactants, are included to obtain the desired properties of the ink to be printable.[15]

Step 1: Binding agent selection and pretest

The selection of a suitable binding agent starts in the first step from literature research on possible binding agent classes.[14,16–18] Utela introduced eight classes: acid/base systems, hydration systems, inorganics, metal salts, organic liquids, phase changing materials, solvents, and in-bed adhesives.[12] In-bed adhesives are unfavorable for the LSD-print process as they tend to increase the slurry viscosity and can be problematic for the slurry stability.

Furthermore, the authors decided to focus on organic binding agents as they can be burnt off or coked so that no undesired impurities are left in the ceramic part. Three types of organic binding agents, namely, polyethyleneimine (PEI), acrylate dispersions, and phenolic resin, were selected in this work as they are stable in water after curing (no dissolution or swelling).

Step 2: Ink formulation

The optimization of the ink formulation consists of several steps. First, to avoid nozzle clogging due to agglomerates, entanglements, or large molecules, the ink is passed through a 5 μm filter.

Furthermore, nozzle clogging during the printing process should already be considered at this stage. In binder jetting, printing is an intermittent phase between layer depositions; therefore, it is essential to ensure that the printhead is not clogging during the pauses between layers.

15512916, 0, Downloaded from https://ceramics.onlinelibrary.wiley.com/doi/10.1111/jace.18951 by Fak - Bam Berlin, Wiley Online Library on [04/01/2023]. See the Terms and Conditions (https://onlinelibrary.wiley.com/terms-and-conditions) on Wiley Online Library for rules of use; OA articles are governed by the applicable Creative Commons License

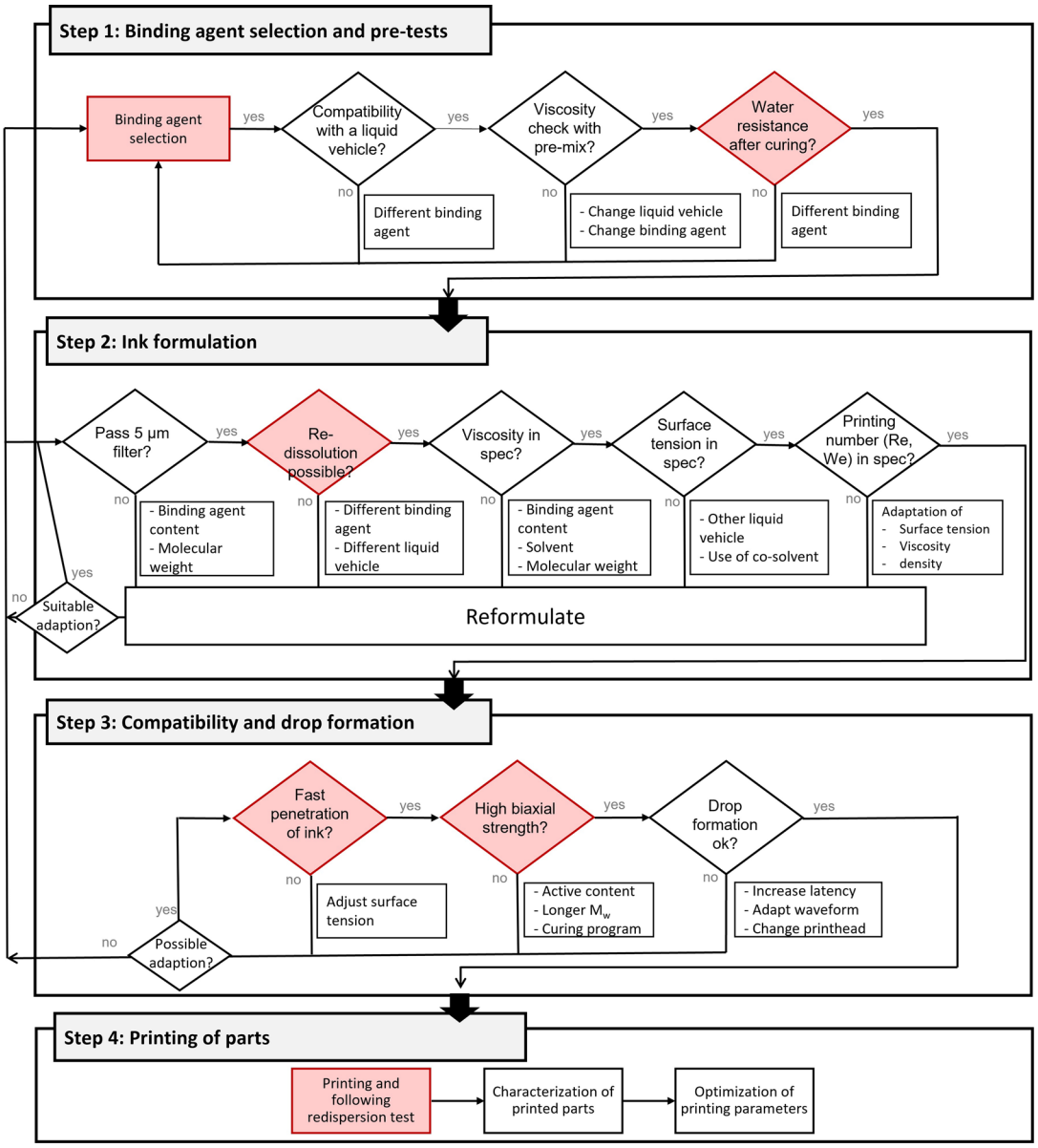

FIGURE 1 Schematic ink development procedure for binder jetting. Steps unique to the layerwise slurry deposition (LSD-print) process are highlighted in red.

This can be achieved by (1) optimizing the ink composition, for example, by using humectants, (2) developing a composition that after drying can quickly be dissolved by the ink itself, or (3) introducing a capping, flushing, or wiping procedure in the printer. In the latter case, a cleaning liquid must be found to effectively dissolve ink residues.

The main physical parameters of the ink are its viscosity, surface tension, and density. A widely used model[19] relates the printability of an ink to the Reynolds number (Re), Weber number (We), and Ohnesorge number (Oh):

$$\mathrm{Re} = \frac{\upsilon \rho a}{\eta} \tag{1}$$

$$\mathrm{We} = \frac{\upsilon^2 \rho a}{\gamma} \tag{2}$$

$$\mathrm{Oh} = \frac{\sqrt{\mathrm{We}}}{\mathrm{Re}} = \frac{\eta}{\sqrt{\gamma \rho a}} \tag{3}$$

$$Z = \frac{1}{\mathrm{Oh}} \tag{4}$$

where υ is the ejection velocity, and a is the nozzle diameter (characteristic length); ρ and η are density and viscosity, and γ is surface tension.

Different criteria have been formulated to predict printability, for example, Derby suggested a printing window for

15512916, 0, Downloaded from https://ceramics.onlinelibrary.wiley.com/doi/10.1111/jace.18951 by Fak - Bam Berlin, Wiley Online Library on [04/01/2023]. See the Terms and Conditions (https://onlinelibrary.wiley.com/terms-and-conditions) on Wiley Online Library for rules of use; OA articles are governed by the applicable Creative Commons License

$1 < Z < 10$.[19] According to this model, for $Z < 1$, viscosity is too high and damps out the pressure pulse, whereas for $Z > 10$, satellite droplets form. Printability is, however, not only determined by the properties of the ink, but also by the selected printing parameters, that is, the waveform of the signal to the piezo actuators.[20,21]

Step 3: Compatibility and drop formation

When the formulation of the ink is finished and its printability is verified, the compatibility with the powder bed material must be tested next.

A general requirement is that the ink wets the powder bed. In this regard, the use of a slurry instead of a powder in the binder jetting process causes further challenges, because the organic additives used in the slurry (dispersant, binders, plasticizers, etc.) can influence the wetting behavior. Poor wetting behavior increases the penetration time and decreases the strength of the printed parts. In a previous work we suggested that, for the LSD-print process, the time evolution of the contact angle of a drop of ink on the powder bed is a simple and effective indicator of wetting behavior.[11] In the current work, we further show that cast specimens prepared from a mixture of slurry and ink can be used as a convenient predictor of the strength of the printed material. It is worth noting that, after any change in the ink composition toward optimizing the compatibility between ink and powder bed, the printability of the ink needs to be validated again.

For this reason, the validation of the predicted printability (step 2) of an ink makes the most sense at the end of step 3. Furthermore, at this point, the printability should be validated by drop-watching tests to evaluate the drop formation behavior for a specific printhead configuration and waveform.[22]

Step 4: Printing of parts

Following steps 1 to 3 allows for minimizing the number of inks that are tested in the binder jetting printer, which typically is the most lengthy and expensive step. Nevertheless, the validation of printing in the actual AM equipment is inevitable to conclude the optimization. In a first printing test, reference geometries for different characterization methods are produced. Typical examples are tablets for biaxial strength measurements. Complex reference geometries are also printed to check for the geometrical accuracy of the print. Specifically for the LSD-print process, only at the end of the process, it can be verified if the printed parts are sufficiently stable to withstand the cleaning step in a water bath.

3 | MATERIALS AND METHODS

In the following, the ink selection procedure summarized in Figure 1 is applied to compare the suitability of three inks for the LSD-print process.

3.1 | Selection of binding agent and pretests

A commercial phenolic resin for binder jetting (PDB, Voxeljet, Germany), a branched PEI ($M_W = 10\,000$, Sigma-Aldrich), and an aqueous polyacrylate dispersion (BYK-LP C25005) were selected for this study.

The PEI 10 000 and the polyacrylate dispersion as-received were too viscous. Thus, for the pretests, both were diluted in deionized water to the desired viscosity range. These mixtures and the phenolic resin were mixed with SiC slurry to produce cast reference specimens, as described elsewhere.[8] Specimens were cast from these mixtures and cured at 130°C overnight to verify if a water-insoluble network is formed.

3.2 | Ink formulation process

To ensure the absence of particles or agglomerates that would clog the nozzles of the printhead, the ink was pushed through a 5 μm syringe filter. Next, a preliminary test was performed to evaluate if dried ink can be dissolved by fresh ink. A thin layer of the ink is spread on a flat aluminum bowl and let dry for 1 h, then a few drops of fresh ink are placed on the dried ink, and it is evaluated if the dried ink dissolves in the fresh ink. Cleaning liquids were tested similarly, but letting the ink dry for at least 24 h instead of only 1 h. Ethylene glycol, ethanol, isopropanol, and a special agent for this purpose called "Cleaner" provided by Zschimmer and Schwarz (Germany) were tested.

Rheology of the inks was characterized with a rotational rheometer (Kinexus Lab+, NETZSCH-Gerätebau GmbH, Germany) at 20°C using a cylinder system according to DIN53015. Viscosity values at a shear rate of 100 1/s were taken for comparison. Surface tension was measured by the pendant drop method using a contact angle goniometer (Goniometer, Ossila, United Kingdom). A single-use pipette with a nozzle diameter of 0.8 mm was used to generate the drop. The density of the different inks was measured by helium pycnometry (Belpycno L, Microtrac, Germany) with a standard deviation of 0.01%.

Following this procedure for adapting the ink, the self-hardening phenolic resin was used without further modification. A PEI-glycerol-water mixture was prepared

15512916, 0, Downloaded from https://ceramics.onlinelibrary.wiley.com/doi/10.1111/jace.18951 by Fak - Bam Berlin, Wiley Online Library on [04/01/2023]. See the Terms and Conditions (https://onlinelibrary.wiley.com/terms-and-conditions) on Wiley Online Library for rules of use; OA articles are governed by the applicable Creative Commons License

with the PEI 10 000. Overall, 20.0 wt% PEI and 3.0 wt% glycerol were mixed in deionized water in an asymmetrical centrifugal mixer (Speedmixer, Hauschild, Germany). The polyacrylate dispersion was diluted to a mixture with 80 wt% binding agent and 20 wt% deionized water.

3.3 | Compatibility and drop formation tests

3.3.1 | Wetting, green strength, and density evaluation

The wettability and therefore the compatibility of the powder bed and the ink were evaluated by contact angle measurements. As the contact angle is difficult to determine for such a rough and porous surface, the contact angle development over time was measured rather than a single value. A 100 μm thick layer of an SiC slurry described by Zocca et al.[8] was spread manually by a blade and let dry in air. This dry layer was placed on the measuring table of the contact angle goniometer, and at least 6 drops with a volume of 1 μl were applied with a microdosing pipette. The contact angle development of each drop over time was recorded, and the average of the contact angles was taken for evaluation.

The SiC slurry was mixed with 6.0 wt% ink, which matches the reference amount of ink that is printed in the green parts in the LSD-print process. This mixture was cast to form tablets with a diameter of 16 mm and thickness of about 4 mm. After casting, the specimens were dried for 5 h at 60°C and cured at 130°C for 16 h. The curing temperature was selected based on a set of preliminary tests, which showed that the maximum green strength of the tablets is achieved at 130°C.

The cast specimens were polished to obtain plane-parallel surfaces for mechanical testing. Printed specimens were already assumed to be plane-parallel, and no grinding was performed on them before testing. The diameter and thickness of each sample were measured with a digital caliper (0.01 mm resolution) in three points and averaged. Specimens were broken according to the ball-on-three-balls method by placing them between one steel ball on one side and three balls each 7 mm in diameter on the other side. The mean values of diameter and thickness were used to calculate the biaxial strength from the peak of the force curve, according to Börger et al.[23]

A testing machine equipped with a 10 kN load cell (Zwick & Roell Xforce HP, Germany) was used with a preload of 5 N and a test speed of 0.3 mm/s. A total of 10 cast specimens and 10 printed specimens for each ink were analyzed. Printed specimens were oriented parallel to the layer plane.

3.3.2 | Drop formation tests

To verify the printability of selected inks, drop-watching experiments were conducted with a Ceradrop F-Printer. The Ceradrop F-Printer was equipped with a Fujifilm Dimatix Spectra SL 128 AA printhead, which was also used in the printing setup, to obtain comparability between the drop-watching experiments and the LSD-print process. The nozzle diameter of this printhead is 50 μm. The setup allows pictures to be taken with a CCD camera and a fully automated drop analysis by the corresponding software.

3.4 | LSD-print and specimen characterization

Printing tests were performed in a custom-built setup. This LSD-print equipment and the printing process are described in detail elsewhere.[7] Green silicon carbide samples were printed by depositing the slurry using a doctor blade, with a layer thickness of 100 μm. Each layer was dried by a flow of hot air from the top and by heating the base plate (approximately at 100°C).

To prevent excessive ink diffusion, each layer was thermally pre-cured by further application of heat before depositing the next layer.

Silicon carbide specimens were printed with the phenolic resin ink and with the PEI ink described in Section 3.2. After printing, the specimens were thermally cured for 16 h at 130°C. De-powdering was performed by placing the build plate with the samples in a water bath and by washing the samples under flowing water. The density and porosity of the green specimens were determined by geometrical measurements and the Archimedes measurement according to DIN-EN-993-1 with deionized water. Microstructure images were taken by scanning electron microscopy (SEM JSM-6490LV, Jeol, Japan).

4 | RESULTS

4.1 | Ink characterization

A preliminary investigation of the three inks allowed determining that all three could pass the 5 μm filter without residues. Furthermore, ethanol was selected as a cleaning liquid for the phenolic ink. For the cleaning of the PEI ink, the Cleaner from Zschimmer and Schwarz was suitable. The polyacrylate dispersion tended to quickly clog the printhead and no suitable cleaning liquid could be found. For this reason, only the PEI and phenolic ink were further investigated in the printing tests (steps 3 and 4, Figure 1).

15512916, 0, Downloaded from https://ceramics.onlinelibrary.wiley.com/doi/10.1111/jace.18951 by Fak - Bam Berlin, Wiley Online Library on [04/01/2023]. See the Terms and Conditions (https://onlinelibrary.wiley.com/terms-and-conditions) on Wiley Online Library for rules of use; OA articles are governed by the applicable Creative Commons License

TABLE 1 Characteristic values of the inks

	Density (g/cm³)	Viscosity at 100 s⁻¹ (MPa s)	Surface tension (mN/m)	Re	We	Oh	Z
Phenolic ink	1.11	11.9	54	37	67	0.22	4.49
PEI ink	1.04	14.5	45	29	73	0.30	3.33
Polyacrylate dispersion	1.03	18.0	30	23	112	0.46	2.17

Abbreviation: PEI, polyethyleneimine.

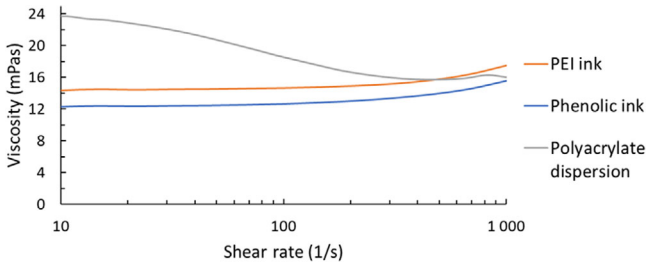

FIGURE 2 Flow curves of the tested inks

Figure 2 shows the flow curves of the three inks. PEI and phenolic ink show Newtonian behavior up to 300 1/s shear rate. For high shear rates, the so-called Taylor–Couette flow occurs, resulting in an apparent increase in viscosity. The viscosity at a shear rate of 100 1/s is similar for both inks with 12 MPa s for the commercial phenolic resin ink and 14 MPa s for the PEI ink. The polyacrylate dispersion ink showed a shear-thinning behavior. Viscosity decreases from almost 24 MPa s to 16 MPa s in the shear rate range from 10 to 1000 1/s.

The measured values of density, viscosity (at 100 1/s), and surface tension of the three inks are shown in Table 1. The characteristic numbers Re, We, Oh, and Z were calculated from these values. The ejection velocity was assumed to be 8 m/s according to the data sheet of the printhead and other references in the literature.[24,25]

The Reynolds and Weber numbers are in a similar range for the phenolic and PEI inks. In contrast, the Weber number for the acrylate ink is 112 and is significantly higher than for the other two inks, whereas the Reynolds number is the lowest of the three. This is related to the higher viscosity and lower surface tension of the acrylate ink compared to the other two. The results are illustrated in Figure 3 in a printability diagram following the model developed by Derby.[19]

4.2 | Compatibility

The compatibility between ink and powder bed was evaluated by measuring the evolution of the contact angle of a drop over time. PEI and phenolic ink drops penetrated the powder bed within less than ten seconds (Figure 4).

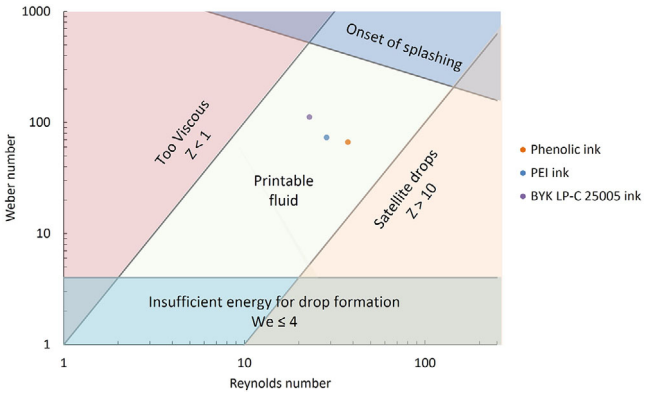

FIGURE 3 Printability diagram for phenolic ink, acrylate ink, and polyethyleneimine (PEI) ink, limits according to Derby (19)

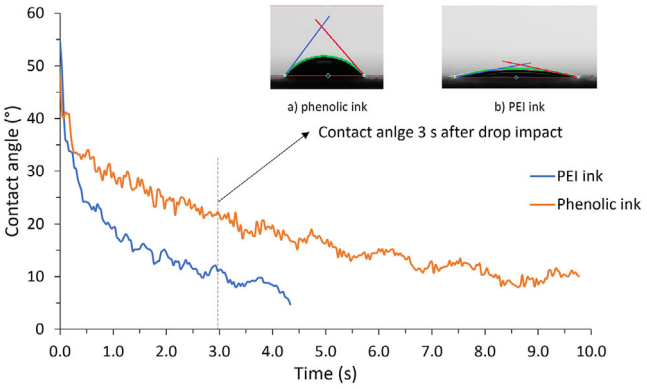

FIGURE 4 Average contact angle over time of the polyethyleneimine (PEI) ink and the phenolic ink on a SiC layer

The phenolic resin penetrates slower than the PEI ink into the powder bed. After about 9 s, the phenolic ink drop forms a 10° angle with the powder bed surface. Contact angles smaller than 10° are difficult to detect correctly on the rough and porous substrate with this measurement setup. Therefore, only the time between the maximum contact angle and a contact angle of 10° was compared. The PEI ink drop shows a contact angle of 10° after about 3.5 s. It has been suggested in our previous work that the comparative behavior of inks in such contact angle measurement can be correlated to their behavior in the printing process.[11]

15512916, 0, Downloaded from https://ceramics.onlinelibrary.wiley.com/doi/10.1111/jace.18951 by Fak - Bam Berlin, Wiley Online Library on [04/01/2023]. See the Terms and Conditions (https://onlinelibrary.wiley.com/terms-and-conditions) on Wiley Online Library for rules of use; OA articles are governed by the applicable Creative Commons License

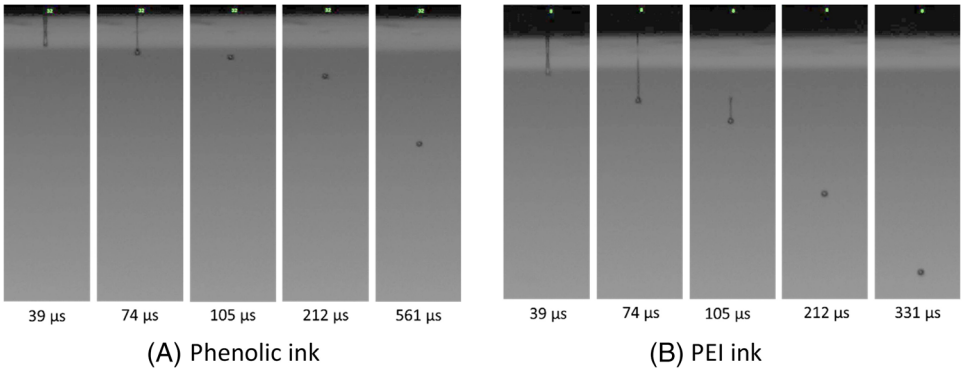

FIGURE 5 Drop formation of the phenolic ink and the polyethyleneimine (PEI) ink (drop volume about 60 pl)

4.3 | Drop watching

The promising evaluation of the inks regarding their We, Re, and Z numbers was generally confirmed by the drop-watching experiments. The drops were ejected with a single-pulse waveform (6 μs at 90 V with 2 μs ramp-up and 2 μs ramp-down) at a frequency of 500 Hz.

The average drop volume was about 60 pl. First, the ink is ejected and stretched out of the nozzle forming a ligament, which is then pinched off from the nozzle and forms a drop. In some cases, a primary drop and satellites are formed which can coalesce to form a single drop before hitting the substrate. For the phenolic ink, no tail formation after pinching of the drop can be seen; therefore, a single drop is formed (Figure 5). The PEI ink instead forms a drop with a long tail, which during the flight retracts into the main drop to form a single drop. Comparing the images in Figure 5A,B, it can be observed that the speed of the ejected drops is lower for the PEI ink compared to the phenolic ink. The last image for the phenolic ink was taken 561 μs after the pulse, and the drop is about halfway between the nozzle and the building platform. The PEI ink drop in contrast has already reached the platform after 561 μs.

It was observed that when using the PEI ink, some nozzles were clogged and did not print reliably after a few times spitting. Flushing and wiping the nozzle plate could restore the printing quality.

4.4 | Printing results

During printing with PEI ink, the printhead had to be flushed several times to restore a good printing quality. The irregular nozzle clogging led to a less homogeneous ink distribution in the part, with visible missing lines.

Specimens printed with PEI ink and phenolic ink were geometrically well defined (see Figure 6). Visually, no difference except for a few missing lines (Figure 6B) due to clogged jets when using the PEI ink could be seen between the specimens printed with the two inks.

4.5 | Strength of printed and cast specimens

Table 2 shows the apparent density and the porosity of the cast and printed specimens. The apparent density was about 2.21 g/cm^3, except for the printed specimens with phenolic resin, which had a density of 2.28 g/cm^3 and lower porosity.

The biaxial green strength of printed and cast specimens with phenolic resin was similar, as shown in Figure 7. The printed tablets with phenolic ink had a Weibull strength of 33 MPa, compared to 29 MPa for the cast material. Moreover, the Weibull moduli of 16 and 20 are in the same range.

A clear difference was noticed instead for the specimens produced with PEI ink. The cast specimens had a green strength of 25 MPa and a Weibull modulus of 37, whereas the printed specimens had a green strength of only 9 MPa and a Weibull modulus of 2.

Figure 8 reveals no significant differences between the microstructure of cast and printed specimens with phenolic ink in the green state. This observation is in agreement with the results of the mechanical characterization. Furthermore, the origin and path of the fracture cannot be identified. Noticeably, there is no visible interface between layers in the fracture surface of the printed specimen (Figure 8B). Comparable results were obtained for the specimen printed with PEI ink. The SEM images appear very similar, as shown in the Supporting Information section.

5 | DISCUSSION

5.1 | Ink selection and printability

A phenolic resin for binder jetting, a branched PEI, and an aqueous polyacrylate dispersion were selected as binding agents for this study. Phenolic resins are already commercially in use for powder-based binder jetting; therefore,

15512916, 0, Downloaded from https://ceramics.onlinelibrary.wiley.com/doi/10.1111/jace.18951 by Fak - Bam Berlin, Wiley Online Library on [04/01/2023]. See the Terms and Conditions (https://onlinelibrary.wiley.com/terms-and-conditions) on Wiley Online Library for rules of use; OA articles are governed by the applicable Creative Commons License

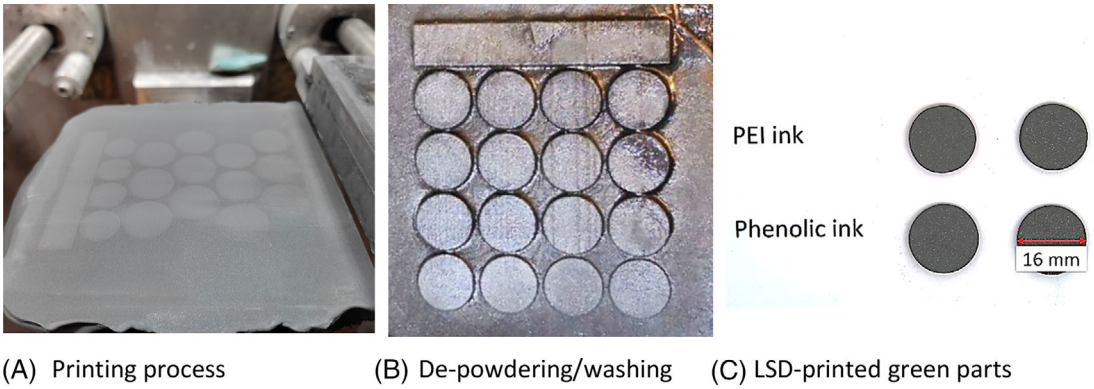

FIGURE 6 Printing of tablets in the layerwise slurry deposition (LSD-print) equipment: (A) printing of the powder bed, (B) de-powdering of the parts by washing the surrounding powder bed in water, (C) printed specimens in the green state with polyethyleneimine (PEI) ink (upper row) and phenolic ink (lower row)

TABLE 2 Apparent density and porosity of printed and cast specimens with polyethyleneimine (PEI) and phenolic ink

Ink	Specimen preparation	Apparent density (g/cm^3)	Total porosity (%)
Phenolic ink	Printed	2.28 ± 0.02	19.8 ± 0.3
Phenolic ink	Cast	2.22 ± 0.03	23.0 ± 1.3
PEI ink	Printed	2.20 ± 0.04	24.2 ± 1.1
PEI ink	Cast	2.21 ± 0.03	23.6 ± 0.9

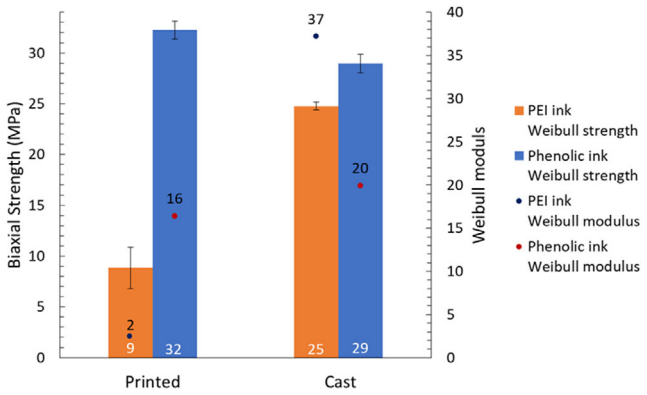

FIGURE 7 Biaxial strength, Weibull modulus, and standard deviation (error bar) of the cast and printed specimens in the green state printed with the phenolic ink and the polyethyleneimine (PEI) ink

this ink is used as a benchmark. PEI has been recently suggested as high-strength binding agent for the binder jetting of sand by Gilmer et al.[26] High molecular weights have higher cohesion, but lower adhesion and often higher brittleness.[27] Furthermore, low molecular weight polymers have a lower viscosity and minimize the risk of crack formation during burnout.[28] Therefore, a PEI with an intermediate molecular weight of 10 000 was selected. The chosen polyacrylate dispersion is a binding agent especially made for ceramic production (BYK-LP C 250025) and is even more environment-friendly, without any warning for harmful ingredients.

According to the literature, all three inks are within the theoretical printability range. This can also be visualized in the printability diagram (Figure 3) according to Derby's model.[19]

For the polyacrylate dispersion, however, no suitable cleaning liquid could be identified. Therefore, no printing trials could be performed due to an irreversible clogging of the printhead. Occasional clogging of the nozzles was observed while printing with PEI ink, which indicates a low latency time, that is, the time that an ink can stay in a jet without showing a change in printing behavior. A possible reason for the low latency time of the PEI ink is most likely its tackiness, which causes the ink to stick to the nozzle plate during firing. A potential solution to this issue could be using a capping station for the printhead to prevent the drying of the ink during the waiting time between layers. Additional strategies to address this issue involve a further optimization of the waveform of the signal for the piezo actuators in the printhead,[29] of the ink composition with humectants,[30] and of the cleaning procedure (sub-jetting and spitting at the end of the print cycle).

According to the experimental study of Dong et al., high viscosity inks show a long time until the break-up of the liquid ligament, as well as a lower speed and drop volume during drop ejection.[31] As the PEI ink has a slightly higher

15512916, 0, Downloaded from https://ceramics.onlinelibrary.wiley.com/doi/10.1111/jace.18951 by Fak - Bam Berlin, Wiley Online Library on [04/01/2023]. See the Terms and Conditions (https://onlinelibrary.wiley.com/terms-and-conditions) on Wiley Online Library for rules of use; OA articles are governed by the applicable Creative Commons License

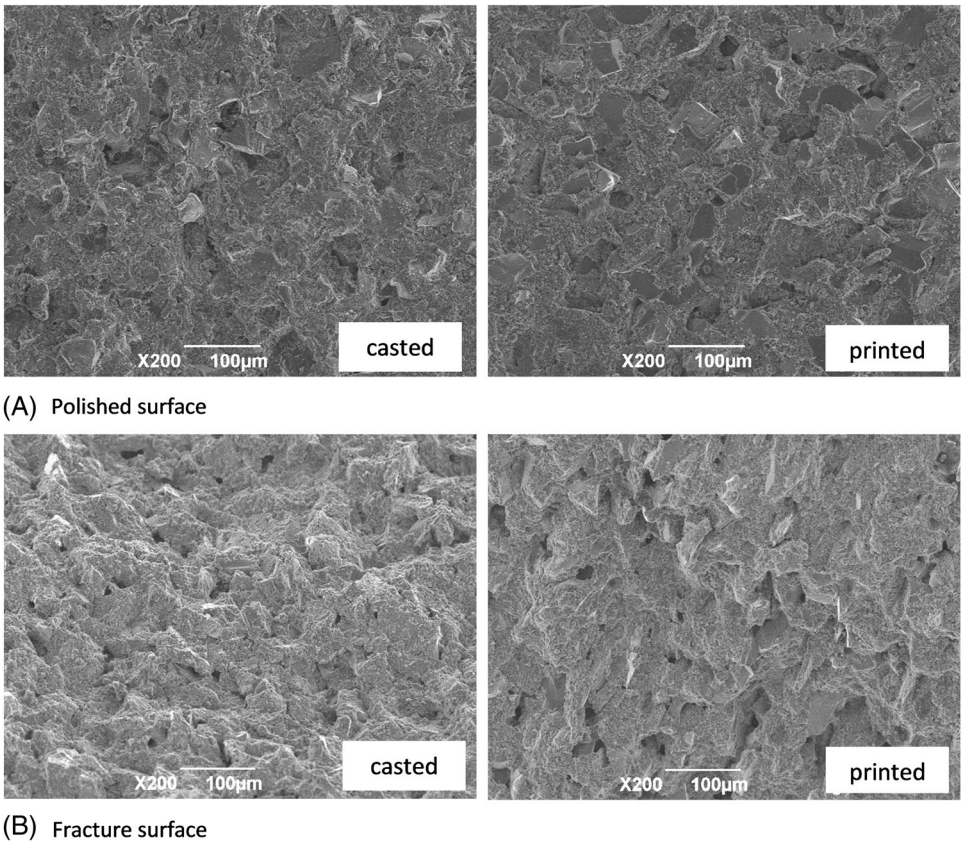

FIGURE 8 Scanning electron microscopy (SEM) images of (A) polished surface and (B) fracture surface of the cast (left) and the printed (right) specimens with phenolic ink

viscosity than the phenolic ink, it was expected that the drop would break-up later from the nozzle plate and has a slower flight speed. It was indeed observed that the PEI ink forms a long-elongated tail. However, the drop flight speed for the PEI ink was slower compared to the phenolic ink. Dong et al. did not consider differences in surface tension and density, which might account for the discrepant observation.[31] Another possible explanation for this could be a different rheological behavior at higher shear rates that could not be measured with the rotational rheometer used in this study. The printhead shear rates between 10^4 and 10^6 1/s occur, which are impossible to reproduce in a standard rotational rheometer.[15,32]

Another parameter that should be taken into consideration is the molecular mass of the polymer molecules in the ink. Long-chain polymer materials tend to form elongated drops, as indeed observed for the PEI with a molecular weight of 10 000 g/mol.[33]

5.2 | Properties of printed and cast specimens

The green strength of the specimens printed with phenolic ink is very high compared to the typical strength specimens printed by the standard powder-based binder jetting process, which is usually in the range of a few MPa. For comparison, a compressive green strength for WC-12% Co parts of 4.2 MPa was measured.[34] Another research work reports a flexural strength of 6.7 MPa for parts made of the commercial Z-Corp ZP102 powder.[35] In a recent publication, Gilmer et al. claimed a high flexural strength using a PEI ink with a sand powder; however, the flexural green strength was limited to 6.2 MPa and was increased up to 53 MPa only after a secondary infiltration step. In comparison, the same authors reported a flexural strength of 3.6 MPa for a commercial furan resin. Lv et al. achieved SiC green parts with a strength of up to 14 MPa using a self-developed thermally initiated cross-linking binding agent based on acrylamide.[30]

In this work, the LSD-printed specimens printed with phenolic resin displayed an outstanding biaxial Weibull strength of 32 MPa (31 MPa mean strength) without any post-processing besides thermal curing. The main reason for the high strength values of the parts made by LSD-print, in contrast to powder-based binder jetting, is likely the higher density of the powder bed itself, and the lower amount of ink needed to form capillary bridges between the particles. Another reason for the high biaxial strength is the good wetting of both inks on the powder and their

15512916, 0, Downloaded from https://ceramics.onlinelibrary.wiley.com/doi/10.1111/jace.18951 by Fak - Bam Berlin, Wiley Online Library on [04/01/2023]. See the Terms and Conditions (https://onlinelibrary.wiley.com/terms-and-conditions) on Wiley Online Library for rules of use; OA articles are governed by the applicable Creative Commons License

chemical surface interaction. The phenolic resin has a large number of polar groups which can form strong bonds on the silica oxide layer which covers the surface of the SiC particles.[2] The PEI ink likewise can form hydrogen bonds with the silica surface. The mechanism for the formation of these hydrogen bonds during curing is described by Gilmer et al.[26]

The PEI ink displayed promising results as an alternative to the phenolic ink, indicating that printing was possible despite some issues related to nozzle clogging. The printing inconsistency due to clogging of the printhead is the most likely explanation for the reduced strength measured on samples printed with the PEI ink, compared to cast samples. Clogged nozzles cause missing lines in the print, which act as preferential weak areas to initiate fracture.

However, as the strengths of the cast specimens for PEI ink and phenolic resin are similar, comparable strength values of the printed specimens can be expected for the PEI ink upon further optimization. In summary, it seems reasonable that cast specimens can be used as a predictor for the strength of printed specimens, as long as nozzle clogging can be avoided during printing. For the PEI ink, a change in the content of glycerol in the ink mixtures might help to reduce nozzle clogging, as in this work, glycerol is mainly used as a humectant. However, it should be considered that glycerol may affect the curing behavior of PEI.[36,37]

Although the focus of this work is on printed green parts, for the production of a ceramic component, the behavior of the printed ink during the thermal post-processing must also be considered. In the case of oxide ceramics, the green parts are typically thermally debinded in air and sintered. Thus, the printed ink should ideally leave no residuals after debinding. In the case of SiSiC, however, the green parts are first coked, a process in which the organic ink is converted to a reactive carbon. The carbon formed during coking plays an important role during the infiltration with liquid silicon, as it reacts with silicon to form secondary silicon carbide. The contribution of the organic ink as carbon source should therefore be taken into account. Phenolic resin is an excellent candidate as binding agent because it is also commonly used as carbon source in silicon carbide slurries.[35,38,39] Figure 9 shows a collection of complex parts printed with an optimal ink (phenolic) and slurry combination. These parts are shown after silicon infiltration, to demonstrate that the material can fully be infiltrated to produce geometrically complex SiSiC ceramic components.

The properties of LSD-printed and infiltrated parts are presented in a previous publication by Zocca et al.,[8] showing that a fully dense SiSiC material with a low amount of residual silicon can be achieved.

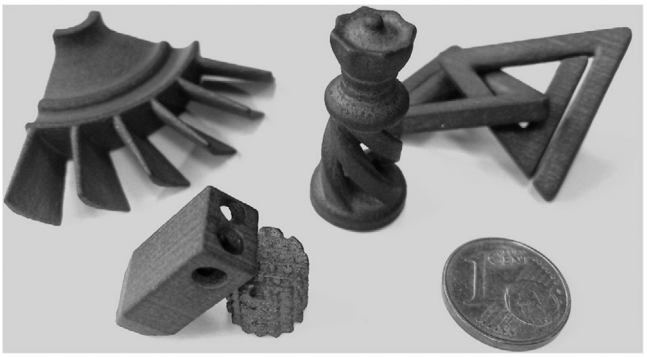

FIGURE 9 SiSiC parts after infiltration showing the capability of the layerwise slurry deposition (LSD-print) process

6 | CONCLUSION

A 4-steps selection and ink development procedure for the LSD-print process, which is a slurry-based variation of binder jetting for ceramics, was presented and validated in this work. In the first step, a binding agent is selected, and its general suitability for the LSD-print process is evaluated by curing and preliminary viscosity tests. At this point, surface tension and viscosity are measured and adapted in an iterative process by using additives in the ink formulation. The interaction of the qualified ink with the powder bed is then tested (step 3) by contact angle measurements and biaxial strength tests. The compatibilities of the ink with the printhead and the drop formation behavior are then investigated in a drop watcher. In the last step, the printing of parts is finally qualified in the binder jetting equipment.

At the current stage of development, only the phenolic resin was proven to be a readily available ink for the LSD-print process. The PEI ink showed promising results, but it should be either further developed or used with a capping station in the equipment. The polyacrylate dispersion ink instead could not be used in binder jetting due to difficulties in redissolving the dried ink with a cleaner.

The procedure introduced in this work was proven to be a helpful guideline for the development of inks for slurry-based binder jetting, considering all crucial aspects that the ink needs to fulfill in the process.

It was shown that an outstanding biaxial strength of 32 MPa could be achieved when using a phenolic resin as printing ink, which is several times higher than the typical strength of parts made by powder-based binder jetting.

ACKNOWLEDGMENTS

Many thanks to Fabrice Rossignol for the management of the AMITIE project and organizing the possibility to do the drop-watching experiments at the Center for Technology Transfers in Ceramics (CTTC) in Limoges. Special thanks

15512916, 0, Downloaded from https://ceramics.onlinelibrary.wiley.com/doi/10.1111/jace.18951 by Fak - Bam Berlin, Wiley Online Library on [04/01/2023]. See the Terms and Conditions (https://onlinelibrary.wiley.com/terms-and-conditions) on Wiley Online Library for rules of use; OA articles are governed by the applicable Creative Commons License

go to Elodie Pereira, Alexis Mayaudon, and Florence Moreau who conducted the drop-watching experiments with the author. This work was supported by EU project AMITIE (Additive Manufacturing for Transnational Innovation in Europe); H2020-MSCA-RISE-2016 EU Research & Innovation Programe, Grant Agreement 734342) and by the German Federal Ministry for Education and Research (BMBF) through grant number 03XP0193.

Open access funding enabled and organized by Projekt DEAL.

ORCID

Sarah Diener https://orcid.org/0000-0002-0675-2671
Andrea Zocca https://orcid.org/0000-0002-0213-2766

REFERENCES

1. Gibson I, Rosen DW, Stucker B. Additive manufacturing technologies: rapid prototyping to direct digital manufacturing. Boston, MA: Springer Science+Business Media LLC; Springer US; 2010.
2. German RM, Bose A. Binder and polymer assisted powder processing. Materials Park, OH: ASM International; 2020.
3. Du W, Ren X, Pei Z, Ma C. Ceramic binder jetting additive manufacturing: a literature review on density. J Manuf Sci Eng. 2020;142(4):1–66.
4. Grau JE, Moon J, Uhland S, Cima M, Sachs E, Sachs E. High green density ceramic components fabricated by the slurry-based 3DP process. Mater Sci. 1997 International Solid Freeform Fabrication Symposium. doi:10.15781/T2DVD80B
5. Sachs E, Cima M, Williams P, Brancazio D, Cornie J. Three dimensional printing: rapid tooling and prototypes directly from a CAD model. J Eng Ind. 1992;114(4):481–8.
6. Sachs EM, Cima MJ, Caradonna MA, Grau J, Serdy JG, Saxton PC et al. Jetting Layers of Powder and the Formation of Fine Powder Beds thereby. Google Patents, US6596224B1.
7. Zocca A, Lima P, Günster J. LSD-based 3D printing of alumina ceramics. J Ceram Sci Technol. 2017;8(1):141–8.
8. Zocca A, Lima P, Diener S, Katsikis N, Günster J. Additive manufacturing of SiSiC by layerwise slurry deposition and binder jetting (LSD-print). J Eur Ceram Soc. 2019;39(13):3527–33.
9. Lima P, Zocca A, Acchar W, Günster J. 3D printing of porcelain by layerwise slurry deposition. J Eur Ceram Soc. 2018;38(9):3395–400.
10. Diener S, Zocca A, Günster J. Literature review: methods for achieving high powder bed densities in ceramic powder bed based additive manufacturing. Open Ceram. 2021;8:100191.
11. Diener S, Schubert H, Held A, Katsikis N, Günster J, Zocca A. Influence of the dispersant on the parts quality in slurry-based binder jetting of SiC ceramics. J Am Ceram Soc. 2022;105:7072–86.
12. Utela BR, Storti D, Anderson RL, Ganter M. Development process for custom three-dimensional printing (3DP) material systems. Journal of Manufacturing Science and Engineering. 2010;132(1):011008.
13. Yanez-Sanchez SI, Lennox MD, Therriault D, Favis BD, Tavares JR. Model approach for binder selection in binder jetting. Ind Eng Chem Res. 2021;60(42):15162–73.
14. Ziaee M, Crane NB. Binder jetting: a review of process, materials, and methods. Addit Manuf. 2019;28:781–801.
15. Magdassi S. Ink requirements and formulations guidelines. In: Magdassi S, editor. The chemistry of inkjet inks. Singapore, Hackensack, N.J: World Scientific Pub. Co; 2010. p. 19–41.
16. Utela B, Storti D, Anderson R, Ganter M. A review of process development steps for new material systems in three dimensional printing (3DP). J Manuf Process. 2008;10(2):96–104.
17. Mostafaei A, Elliott AM, Barnes JE, Li F, Tan W, Cramer CL, et al. Binder jet 3D printing—process parameters, materials, properties, modeling, and challenges. Prog Mater Sci. 2021;119:100707. [cited 2021 Jan 23].
18. Lv X, Ye F, Cheng L, Fan S, Liu Y. Binder jetting of ceramics: powders, binders, printing parameters, equipment, and post-treatment. Ceramics International. 2019;45(10):12609–24. Available from: URL: http://www.sciencedirect.com/science/article/pii/S0272884219308223
19. Derby B. Inkjet printing of functional and structural materials: fluid property requirements, feature stability, and resolution. Annu Rev Mater Res. 2010;40(1):395–414.
20. Liu Y-F, Tsai M-H, Pai Y-F, Hwang W-S. Control of droplet formation by operating waveform for inks with various viscosities in piezoelectric inkjet printing. Appl Phys A. 2013;111(2):509–16. Available from: URL: https://link.springer.com/article/10.1007/s00339-013-7569-7
21. Aqeel AB, Mohasan M, Lv P, Yang Y, Duan H. Effects of the actuation waveform on the drop size reduction in drop-on-demand inkjet printing. Acta Mech Sin. 2020;36(5):983–9. Available from: URL: https://link.springer.com/article/10.1007/s10409-020-00991-y
22. Versluis M. High-speed imaging in fluids. Exp Fluids. 2013;54(2):1–35.
23. Börger A, Supancic P, Danzer R. The ball on three balls test for strength testing of brittle discs: stress distribution in the disc. J Eur Ceram Soc. 2002;22(9–10):1425–36.
24. Fujifilm Dimatix. SL-128 AA [cited 2021 Nov 25]. Available from: URL: https://asset.fujifilm.com/www/us/files/2020-03/8f6f46b197b6cb8746cf5a6c163fe08f/PDS00008.pdf
25. Yarin AL. Drop impact dynamics: splashing, spreading, receding, bouncing. Annu Rev Fluid Mech. 2006;38(1):159–92.
26. Gilmer DB, Han L, Lehmann ML, Siddel DH, Yang G, Chowdhury AU, et al. Additive manufacturing of strong silica sand structures enabled by polyethyleneimine binder. Nat Commun. 2021;12(1):5144.
27. Schwalm R. UV coatings: basics, recent developments and new applications. Amsterdam, London: Elsevier Science; 2006. Available from: URL: http://www.sciencedirect.com/science/book/9780444529794
28. Brigo L, Schmidt JEM, Gandin A, Michieli N, Colombo P, Brusatin G. 3D nanofabrication of SiOC ceramic structures. Adv Sci (Weinh). 2018;5(12):1800937.
29. Pond SF. Inkjet technology and product development strategies. Carlsbad, Calif: Torrey Pines Research; 2000.
30. Lv X, Ye F, Cheng L, Zhang L. A versatile thermally initiated crosslinking binder for additive manufacturing of strong structures. Addit Manuf. 2022;56:102893.
31. Dong H, Carr WW, Morris JF. An experimental study of drop-on-demand drop formation. Phys Fluids. 2006;18(7):72102.

15512916, 0, Downloaded from https://ceramics.onlinelibrary.wiley.com/doi/10.1111/jace.18951 by Fak - Bam Berlin, Wiley Online Library on [04/01/2023]. See the Terms and Conditions (https://onlinelibrary.wiley.com/terms-and-conditions) on Wiley Online Library for rules of use; OA articles are governed by the applicable Creative Commons License

32. Reis N, Ainsley C, Derby B. Ink-jet delivery of particle suspensions by piezoelectric droplet ejectors. J Appl Phys. 2005;97(9):94903.
33. Anna SL, McKinley GH. Elasto-capillary thinning and breakup of model elastic liquids. J Rheol. 2001;45(1):115–38.
34. Enneti RK, Prough KC. Effect of binder saturation and powder layer thickness on the green strength of the binder jet 3D printing (BJ3DP) WC-12%Co powders. Int J Refract Met Hard Mater. 2019;84:104991.
35. Vaezi M, Chua CK. Effects of layer thickness and binder saturation level parameters on 3D printing process. Int J Adv Manuf Technol. 2011;53(1–4):275–84.
36. Ghriga MA, Grassl B, Gareche M, Khodja M, Lebouachera SEI, Andreu N, et al. Review of recent advances in polyethylenimine crosslinked polymer gels used for conformance control applications. Polym Bull. 2019;76(11):6001–29.
37. Singh B, Maharjan S, Park T-E, Jiang T, Kang S-K, Choi Y-J, et al. Tuning the buffering capacity of polyethylenimine with glycerol molecules for efficient gene delivery: staying in or out of the endosomes. Macromol Biosci. 2015;15(5):622–35.
38. Miyanaji H, Yang L. Equilibirium Saturation in Binder Jetting Additive Manufacturing Processes: Theoretical Model vs. Experimental Observations. In: Proceedings of the 27th Annual International Solid Freeform Fabrication Symposium. 2016. [cited 2020 Sep 1].
39. Mao Y, Li J, Li W, Cai D, Wei Q. Binder jetting additive manufacturing of 316L stainless-steel green parts with high strength and low binder content: Binder preparation and process optimization. J Mater Proc Technol. 2021;291:117020.

SUPPORTING INFORMATION

Additional supporting information can be found online in the Supporting Information section at the end of this article.

How to cite this article: Diener S, Schubert H, Günster J, Zocca A. Ink development for the additive manufacturing of strong green parts by layerwise slurry deposition (LSD-print). J Am Ceram Soc. 2023;1–12.
https://doi.org/10.1111/jace.18951

15512916, 0, Downloaded from https://ceramics.onlinelibrary.wiley.com/doi/10.1111/jace.18951 by Fak - Bam Berlin, Wiley Online Library on [04/01/2023]. See the Terms and Conditions (https://onlinelibrary.wiley.com/terms-and-conditions) on Wiley Online Library for rules of use; OA articles are governed by the applicable Creative Commons License